Current Research in Green and Sustainable Chemistry 4 (2021) 100212

Contents lists available at ScienceDirect

Current Research in Green and Sustainable Chemistry

journal homepage: www.elsevier.com/journals/current-research-in-green-and-sustainable-chemistry/2666-0865

Green synthesis silver nanoparticles *via Eichhornia Crassipes* leaves extract and their applications

Leena V. Hublikar [a,c], Sharanabasava V. Ganachari [b,*], Narasimha Raghavendra [c], Veerabhadragouda B. Patil [d], Nagaraj R. Banapurmath [b]

[a] Department of Chemistry, KLE Technological University, Vidyanagar, Hubballi, 580031, India
[b] Centre for Material Science, School of Mechanical Engineering, KLE Technological University, Vidyanagar, Hubballi, 580031, India
[c] Department of Chemistry, KLE Society's P. C. Jabin Science College (Autonomous) Vidyanagar, Hubballi, 580031, India
[d] Institute of Energetic Materials, Faculty of Chemical Technology, University of Pardubice, Czech Republic

ARTICLE INFO

Keywords:
Silver nanoparticles
Antibacterial
Anticorrosion
Tafel plot
High-resolution transmission electron microscopy

ABSTRACT

Recent times sustained efforts have been made in the bottom-up approach and biological Ag nanoparticles synthesis, in present work synthesized silver nanoparticles *via* green synthesis from the *Eichhornia crassipes* (EC) leaf extract AgNPs at room temperature with pH of 10–12. Synthesized AgNPs characterized thoroughly for phase purity and morphology by various characterization techniques. Phytochemical activities of *Eichhornia crassipes* (EC) leaf extract were shown that main constituents flavonoids, quercetin enhances the conversion of Ag^{+} to Ag^{0}. This is also confirmed through the electronic property (E_{HOMO} and E_{LUMO}) of EC leaf extract, which was analyzed through quantum chemical studies. Further the antibacterial activity of AgNPs was screened on *E. coli and S. aureus*. The result reveals that AgNPs has good antibacterial properties towards the bacteria *E. coli*. The AgNPs is dedicated also in testing the effectiveness of aluminum corrosion in the acid system at room temperature using Tafel plots, atomic absorption spectroscopy, and AC impedance spectroscopy techniques. Corroded aluminum pieces were observed by using the SEM technique.

1. Introduction

In the last few years, research focus shifted more towards Nobel metal nanoparticles due to their enormous applications in environmental, biomedical, and electrochemical sciences. However, the hazardous chemical methods of synthesis of nanoparticles made researchers keep pausing for their thoughts towards exploring novel nanoparticles through chemical synthesis methods. At the same time, waste management is the big task, which is out of reach to the scientist. Hence, investigation of the environmentally benign route for the synthesis of nanoparticles is vital to sustain the environment by reaching the alternate method for the chemical nano-synthesis and management of the waste. Then, an environmentally safe plant-mediated biological method was given the bottom-up approach of novel nanoparticles green synthesis. Phyto mining is the process of conversion of metal ions into metal nanoparticles using phytochemicals content in plant extract. Green synthesis in comparison to Chemical synthesis, have biocompatibility as generally they got reduction property to reduce ions into atoms of nano-size without the involvement of noxious and harmful chemicals [1]. The green chemical approach of nanoparticle synthesis gave a hint for molecules which are biologically active from plant extract responsible for reducing and stabilizing the process [2]. Nanoscale provides a greater surface to volume ratio which makes them to implement in various fields such as drug delivery [3] micro - electronics [4] antimicrobial property [5], diagnosis, catalysis [6], anticorrosion, bio-fertilizer [7], bio-mimicking, nano--sensing, polymer nanocomposites, and super hydrophobicity [8]. Using bismuth, niobium, and iron photocatalysts ($Bi_2FexNbO_7$) and a "green technique" based on *S. trilobata* leaf paste for environmental applications [9,10]. In addition, nanostructure species are explored in numerous fields such as energy [11], food, agriculture, biotechnology, textile [12], medicine and environment [13].

Green is a word used to emphasize the use of plant sources in the synthesis of nanoparticles. Furthermore, traditional synthetic strategies are employed in this synthesis, which is an environmentally friendly method i.e., water hyacinth is considered invasive, treated as major waste for aquatic, is used in this synthesis. Thus, this must be considered as waste material used to synthesis the nanoparticles [14] The solvent medium, reducing agent, and capping agent to stabilize the nanoparticles

* Corresponding author.,
E-mail addresses: sharanu14@gmail.com, sharanabasava@kletech.ac.in (S.V. Ganachari).

https://doi.org/10.1016/j.crgsc.2021.100212
Received 28 August 2021; Received in revised form 29 October 2021; Accepted 2 November 2021
Available online 10 November 2021

Table 1
Methods of corrosion control.

Control method	Description
Corrosion inhibitors	These are chemical substances introduced in small concentrations to a corrosive system to reduce electrochemical process.
Electrical protection	The metal corrosion can be prevented by making small potential difference between anode and cathode.
Excellent Equipment Design (EED)	EED prevents the corrosion of metals by avoiding the two dissimilar metal connections in the corrosive solution.
Surface coating	It involves use of protective coatings to generate physical barrier between metal and corrosive system.
Material selection	The metal having high mechanical strength should be selected.

have a key role in biological synthesis [15] and helps environmental toxic content removals [16].

The microbial infection efficacy, resistance towards antibiotics, and increasing mutation rate made the green nano-synthesis a worth. Bio-molecules of plants like macromolecules, micro molecules and natural metabolites (proteins, amino acids, alkaloids etc.) play key roles in developing scientific potential choice for the study of synthesis and structural modifications of AgNPs. Many silver nanoparticles (silver, gold, zinc, etc.) are synthesized by using plant portion extracts [17]. Physical and chemical methods of synthesizing nanoparticles [18] have limited advantages due to their high noxious nature. The method needs high energy input and costly due to the down streaming process [19]. As reported in the previous articles, green chemistry is a safe and costeffective method. The Silver nitrate is a precursor for synthesizing AgNPs and secondary metabolites and phytocompounds necessary for reducing Ag^{+} to Ag^{0}. But the biosynthesis of same silver nanoparticles with different applications, in biological as well as electrochemical is not being reported. However, biosynthesis of silver nanoparticles with different applications are being reported in the field of anticorrosion activities applications [20]. Cow urine is used as reducing agent for Ag nanoparticles. Bio-synthesized Ag nano-particles are potent catalyst for organic transformation reactions. They have been successfully used as a photocatalyst for the degradation of hazardous organic dyes such as methylene blue and crystal violet [63]. A species of aquatic plant that is invasive and causes impairment (damage) to the environment and human health is known as the *E. coli* bacteria (EC) [21–24]. This is considered as biomass for generating energy sources, fertilizers, animal feeds, water treatment, and biopesticide [25] Belonging to the family *Pontendericeae*, its plant taxonomy shows that, walls of these cells are composed of ferulic acid.

Ferulic acid (FA), a universal available normal phenolic chemical present in different plant sources as leaves, seeds in free form or in conjugated form. Plant cell walls also contain lignin, polysaccharides, polyamines, and glycoproteins. This emphasis on a wide range of phytochemical properties, including antimicrobial, anticarcinogenic, antiallergic, antioxidant, and antiinflammatory properties [26], improves sperm viability [27]. Along with acts as astonishing antiviral, metal chelation, gene expression and signal transduction, modulation of enzyme [28–32].

Many research articles reveal the antibacterial activity of silver nanoparticles, which motivated us to determine this property of AgNPs. The bacterial activity of AgNPs was studied with *E. coli* and *S. aureus* bacteria and the results are discussed in this paper. Further, aluminium (Al) corrosion is an electro-chemical reaction in the active parts of it in the hydrochloric acid system when exposed to corrosive chemicals [33]. Al metal is used in chemical processing, nuclear power, transportation, and the construction of pipelines. Different technologies were used to prevent the Aluminium corrosion process, such as corrosion inhibitors, cathodic protection, anodic protection, coatings, and paintings. Corrosion inhibitors are preferred due to their easy installation and effective efficiency in metal corrosion protection [21,34–37]. Hydrochloric acid solution is widely used in industry to remove impurities from metal surfaces. Over the time, the high usage of hydrochloric acid solution causes disintegration of the Al surface. Hence, nowadays, the academic and industry sectors are interested in using inhibitors due to the high adsorption rate. The adsorption process mainly depends on the inhibitor species physical, chemical properties, activeness of the Al, the corrosive solution, temperature, and electrochemical potential in the AlHCl solution-metal line edge and more. Environmental policies and legislation enforce a restriction on the usage of synthetic corrosion inhibitors as they are toxic to the environment, which causes a rise in the cost of several industrial units. This motivates the discovery of effective and zero toxicity corrosion inhibition species [13,22,38–42]. Table 1 provides information about the methods of corrosion control. The effectiveness of tailored nanoparticles is understood by knowing their structure, by maintaining precursor and reaction conditions.

Fig. 1. Actual photographs of *Eichhornia Crassipes* taken at Unkal Lake Hubballi, Karnataka INDIA GPS location 15.374464, 75.102985.

Table 2
Qualitative analysis of Phytochemical results shown by EC leaf extract.

Sl.No	Test	Observation	Inference
I a.	Qualitative Analysis: Test for Alkaloids		
1.	Mayer' s test: *Eichhornia crassipes* EC leaf extract + Mayer's reagent	white creamy precipitate	Presence of Alkaloids are confirmed
2.	Wagner's test: *Eichhornia crassipes* EC leaf extract + Wagner"s reagent	reddish-Brown precipitate	Presence of Alkaloids are confirmed
I·C.	Qualitative Analysis: Test for Carbohydrates		
1.	Molish' s test: *Eichhornia crassipes* EC leaf extract + α- naphthol in alcohol, two drops + concentrated sulphuric acid	No violet ring	presence of carbohydrates.
2.	Benedict' s test: *Eichhornia crassipes* EC leaf extract + Benedict"s reagent heated on a boiling water bath	coloured precipitate	presence of sugar
I·F.	Qualitative Analysis: Phenolic compounds		
1.	Ferric Chloride test *Eichhornia crassipes* EC leaf extract +5 ml of distilled water +5% ferric chloride solution	No dark green colour	phenolic compound may be preset
2.	Lead acetate test *Eichhornia crassipes* EC leaf extract +5 ml of distilled water +10% lead acetate solution	bulky white precipitate	phenolic compounds may be preset
3.	Alkaline reagent test *Eichhornia crassipes* EC leaf extract +10% ammonium hydroxide solution	Yellow fluorescence	flavonoids may be preset
	Qualitative Analysis: Test for phytosterols		
1.	Libermann-Burchard's test *Eichhornia crassipes* EC leaf extract +2 ml acetic anhydride+ 2 drops of concentrated sulphuric acid	No array of colour change	Absence of phytosterols
I·H.	Qualitative Analysis: Test for Proteins		
1.	Millon's test *Eichhornia crassipes* EC leaf extract +2 ml of Millon"s reagent	No white precipitate	Absence of proteins

The green nano particles obtained from the plant species expected to show good corrosion protection property for many metals in different corrosive media, at acidic or basic medias and at different concentrations of them. However, no specific report on EC as an anti-corrosion stuff for Al metal in 1 M HCl solution. Keeping this in mind, in this study, silver nanoparticles were synthesized by extracting the leaves of the EC plant. The synthesis of EC extract silver nanoparticles was confirmed by studies in the ultraviolet/visible, FT-IR, PXRD, and HRTEM. The corrosion inhibition efficiency of EC was determined by using alternating current impedance spectroscopy. The corrosion inhibition efficiency of silver nanoparticles was tested with Atomic Absorption Spectroscopy (AAS) and electrochemical techniques.

2. Materials and methods

Eichhornia crassipes is a floating aquatic plant (Fig. 1), usually grows in shallow freshwater ponds, lakes, and rivers. It grows vigorously within 15–20 days and forms a dense, floating mat, over the surface of water bodies. Fresh leaves of *Eichhornia crassipes* were gathered from the local area (Unkal lake) of Hubballi, Karnataka. The plant leaves were convincingly cleaned with deionised water to remove the debris that may contaminate the extract and finally dried over under the sun rays. The dried leaves were crushed using agate mortar and pestle. The Soxhlet extraction was performed with 50 g of plant species (dried leaves) powder in the 300 ml of acetone for about 7 h. After that, the extracted green coloured chemical was filtered and stored in the refrigerator to prevent side reactions and contamination-free.

2.1. Phytochemical analysis

Biological synthesis of nanoparticles employs a bottom-up method in which carried out by the participation of reducing and stabilizing agents. Various phyto-moieties present in the extracts of EC leaf are reported by phytochemical analysis. Table 2 lists the results of the qualitative analysis screening tests that were conducted in their laboratory for this purpose.

These phytomedicinal compounds plays stimulating character act as mild reducing agent in the silver nitrate (Ag^{+}) to silver (Ag^{0}) in nano-size. Also represents itself as capping and stabilizing agent. The phyto-chemical analysis of *eichhornia cracippes* leaves also showed the presence of alkaloids, terpenoids, phenolics, flavonoids and tannins. As reported earlier, the phenolic content of water hyacinth contains a good quantity of quercetin and is reported the highest content of flavonoids also [43].

Material resources which protect the cells from unstable free radicals, are called as antioxidants. The flavonoid contents help to reduce risk of cardiovascular diseases and different cancers. Especially Quercetin, a plant pigment is a potent antioxidant flavonoid. It is a useful antioxidant which possess a protective ability against various drug toxicities [44].

Major content of the phytochemicals found to be Flavonoid (quercetin). The hydroxyl (OH) groups of flavonoids (quercetin) are responsible for reducing silver ions into silver in nano-size. Tautomer are structural isomers formed by transferring protons from one site to another in the molecule. Quercetin exhibits keto-enol isomerism. Hydrogen atom released during this conversion of enol to keto forms in quercetin helps convert the ion into metallic silver nanosized and stabilizes the AgNPs.

2.2. Synthesis of AgNPs

The AR grade silver nitrate was purchased of the brand SDFCL, Mumbai, in double distilled water its solution is prepared. The 1:4 ratios of precursor and plant extract, $AgNO_3$ (0.01 N) of 200 ml, were added to the 50 ml of EC extract. The pH plays important role in the synthesis of nanoparticles. The colour intensity of the aqueous solution also varied with alkaline pH of 9–11 is appropriate for the synthesis. Here in this pH of solution by EC extract found to be 11 and a lower concentration of silver nitrate is prepared to facilitate its hidden properties to explore. After mixing and agitation of the reaction mixture, it was placed in the sunlight for about 15 min.

The colour was changes from green to light brown to dark brown gives a clear hint of the formation of *Eichhornia crassipes* (EC) extract silver nanoparticles or green silver nanoparticles (Fig. 2). These green nanoparticles were kept in the centrifuge tubes and centrifugation was performed for about 20 min at 1000 rpm. After that, the colourless centrifugate is discarded and brown coloured residue left is transferred into a clean China dish. The residue is dried over the hot plate at a lower temperature carefully to avoid the charring of the residue (see Fig. 3).

2.3. Characterization of AgNPs

Prime techniques incorporated to characterize *Eichhornia crassipes* (EC) extract are as follows, AgNPs were screened with UV–Visible spectroscopy on LABMAN LMSP-UV1200 with a wavelength accuracy of +0.5 nm. Fourier-transform infrared spectroscopy (FT-IR) study was performed to confirm the formation of green silver nanoparticles in the range of 4500–400 cm^{-1} by instrumentation at Sophisticated Analytical Instrumentation Facilities (SAIF) Centre Karnatak University, Dharwad

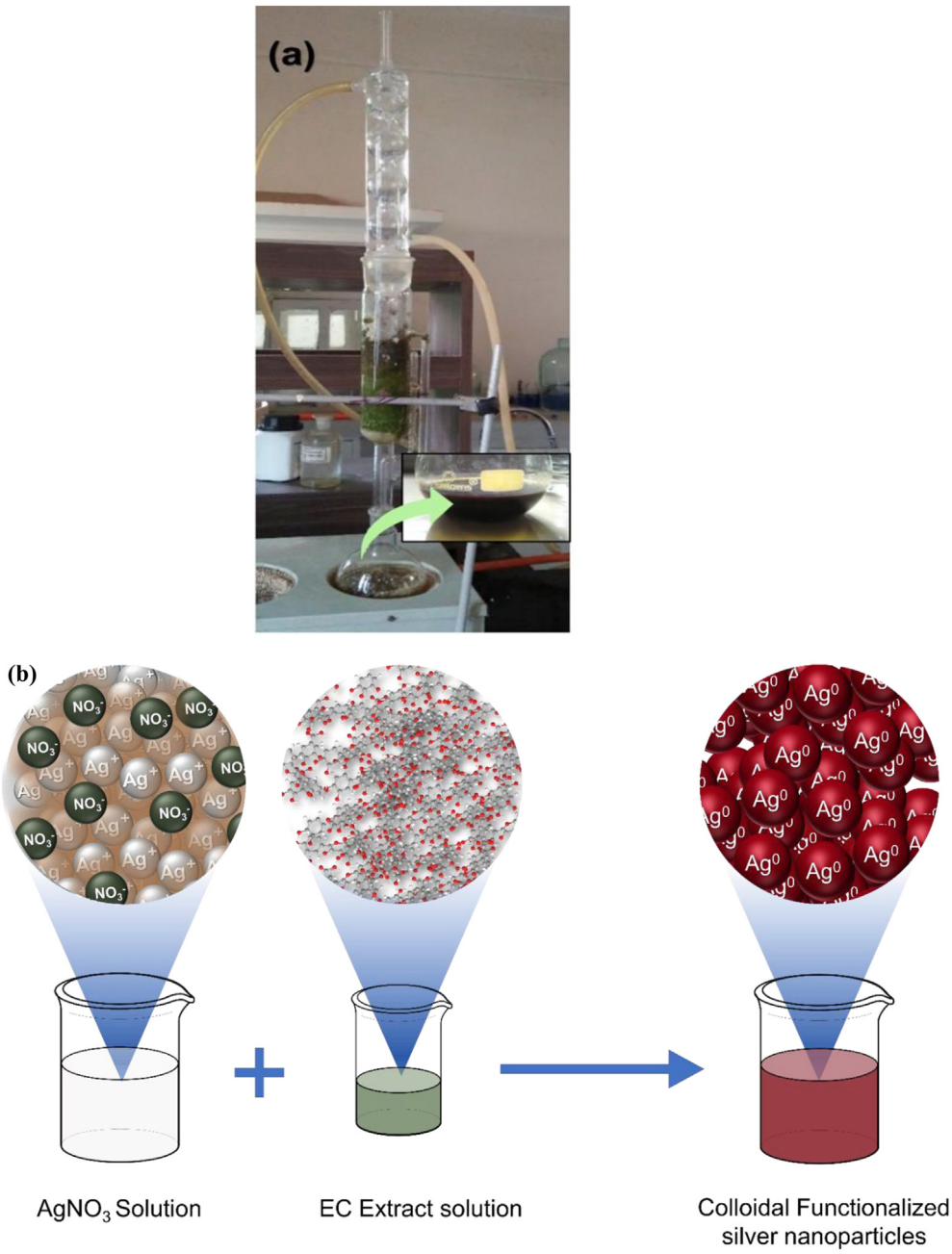

Fig. 2. a) Experimental setup of synthesis of plant extract -Soxhlet apparatus b) schematic flow of green synthesis of AgNPs by EC leaf extract. (For interpretation of the references to colour in this figure legend, the reader is referred to the Web version of this article.)

(KUD) India by using NICOLET 6700, USA instruments. X-ray Powder Diffraction (X-RD) of model Xpert MPD, make Philips, Holland was used to analyze the structure of the newly synthesized AgNPs. The XRD patterns were recorded on X-ray diffractometer at the range of 2θ from 3° to 136° using Cu target X-Ray tube, Cu Kα (λ = 1.5406 A) radiation with a tracking voltage of 40 KV. Scanning Electron Microscopy (SEM-EDX) was carried out to learn the external morphology of AgNPs. To analyze morphological features of AgNPs, field emission scanning electron microscope was also used at an accelerating voltage with LaB6 filament 2 nm 30 KV with W filament 3.5 nm at 30 kv by emission current of 0–200 μA and accelerating voltage: 0.2 to 30 kv. The size, shape, and morphology of synthesized AgNPs, were confirmed using HR-TEM (model: Thermo Scientific, Model: TALOS F200S G2, 200 KV, FEG, performed in TEM Lab, Centre for Nano and Soft Matter Sciences (CeNS), Bengaluru.

2.4. Theoretical studies

Quantum chemical studies were carried out for Gallic acid and Quercetin, which are considered key EC extract components. Different quantum chemical parameters obtained from quantum chemical studies provide essential information about the nature of the electron transfer property of Gallic acid and Quercetin. Therefore, in the present investigation, a theoretical study was performed by using the Argus Lab (advance version) software through PM3 method (Table 3 and Fig. 4(a–d)).

2.5. Antibacterial studies

As per earlier reports, silver nanoparticles derived from plant sources exhibited significant antibacterial activity. The antibacterial activity of

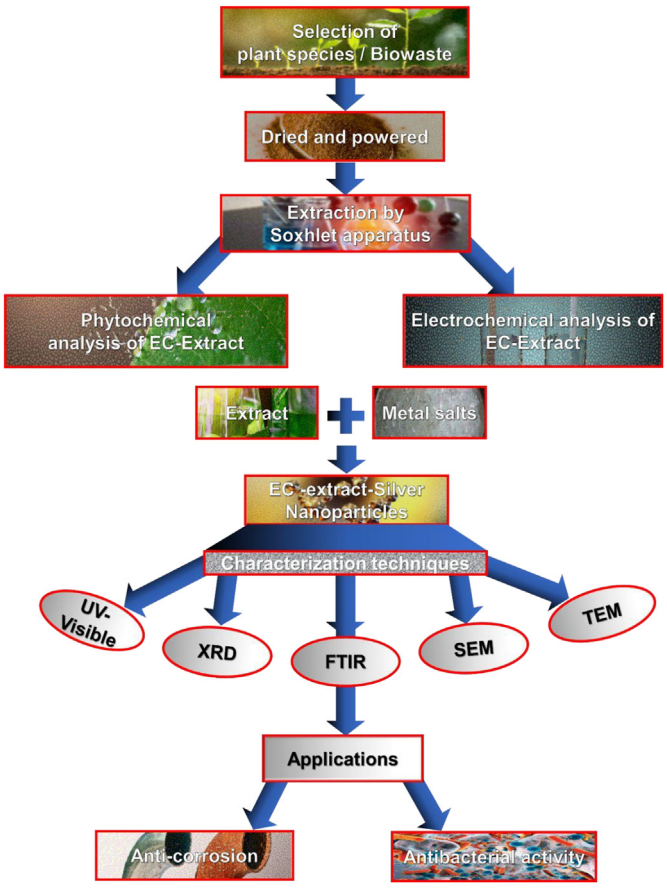

Fig. 3. Schematic illustration of synthesis, characterization, and applications of EC leaf extract silver nanoparticle.

EC synthesized AgNPs against gram-positive and gram-negative bacteria (*E. coli and S. aureus*) was observed at the Biogenics Research and Training Centre in Biotechnology Veena plaza, P. B Road, Hubli-580,031. The agar diffusion method was used to conduct the analysis, and the zone of inhibition was measured in the process. The solvent used is DMSO, and the antibiotic used is IC Ciprofloxacin, which is a standard antibiotic. Initially, the stock cultures of bacteria were grown in broth media at 37 °C for 18 h, and then they were transferred to the test tube. The agar plates and wells in the plate were made from the above-mentioned media. During that time, each plate was protected for 18 h. Plates were filled with nano-samples in a variety of volumes with a 20-min gap between each plate filling. Further plates were incubated at 37 °C for 24 h to determine the diameter of the inhibition zone, which was measured in mm.

2.6. Corrosion test methods

During the current investigation, Al metal of type Al-63400 with chemical compositions of Cu (0.1%), Mg (0.4%–0.9%), Fe (0.2%), Zn (0.2%), Mn (0.3%), Tl (0.1%), Cr (0.2%), and Si (0.7%) was used for corrosion studies [47].

For both Tafel plot and AC impedance spectroscopy technique, 1 cm^2 of Al metal pieces were exposed to the corrosive system and remaining portion covered with epoxy resin. Prior to test, the metal pieces wash polished with sandpapers and washed with acetone. The chemical (atomic absorption spectroscopy) and electrochemical (Tafel plot and AC impedance spectroscopy) techniques were used to evaluate the inhibitory efficacy of AgNPs against metal corrosion on the Al surface in the 1 M HCl solution. Surface studies of Al in 1 Molar HCl solution were carried out using the SEM technique, both without and with the optimal concentration of AgNPs present. The Al (III) ion concentration in the 1 M HCl solution was determined using atomic absorption spectroscopy (AAS) using the model GBC, 908 and AgNPs at concentrations ranging from 1 mg/L to 4 mg/L. One centimetre of polished Al metal was exposed for a total of 10 h for this purpose. Al is then removed from the corrosive solution and allowed to dry before being weighed to determine the amount of weight loss. The protection efficiency can be calculated as per the following expression.

$$Protection\ efficiency\ (\%) = \frac{(B-A)}{B} \times 100 \quad (1)$$

where, B-Amount of dissolved Al (III) content without AgNPs and A-Amount of dissolved Al (III) content with AgNPs.

Electrochemical calculations were achieved using a CHI 660C workstation with the help of three electrodes (platinum, calomel and working cell (Al)). The AC impedance spectroscopy technique was conducted on 105- 102 Hz frequency after the stabilization period of 30 min. The potential of −0.20 to +0.20 V versus open circuit potential (OCP) at the scan rate of 1 mV/s is employed for the potentio-dynamic polarization (Tafel plots). Tafel slopes, and corrosion potential (Ecorr) values were obtained from inbuilt software of CH instrument. The corrosion current density values were used to evaluate the polarization resistance (Rp) values with the help of Stern-Geary equation [48].

Protection efficiency can be calculated from the charge transfer resistance (from AC impedance study) and Aluminium corrosion current density (from potentiodynamic polarization) according to this expression.

$$Protection\ efficiency(\%) = \frac{1 - R^0_{ct}}{R_{ct}} \times 100 \quad (2)$$

where, Rct 0 = Charge transmission resistance value without AgNPs and Rct = Charge transfer resistance value with AgNPs.

$$Inhibition\ efficiency(\%) = \frac{1 - I_{corr}}{I^0_{corr}} \times 100 \quad (3)$$

Table 3
Quantum chemical results of higher amount of ingredients of the EC leaf extract which are acting as mild reducing agent AgNPs synthesis [45].

Name of medicinal compound	HOMO (eV)	LUMO (eV)	Energy gap (eV)	I	A	H	χ	Σ	M	Ω
Gallic acid	-9.1346	-2.0261	-11.160	9.134	2.0261	3.5542	5.580	0.281	-5.5803	4.380
Quercetin	-9.783	-1.840	-11.623	9.783	1.840	3.971	5.813	0.251	-5.813	4.254

The different quantum chemical parameters such as HOMO, LUMO, electronegativity (χ), electrophilicity index (ω), Chemical softness (σ), electron attraction (A), chemical potential (μ), ionization potential (I), and chemical hardness (η) calculated as per the literature [46].

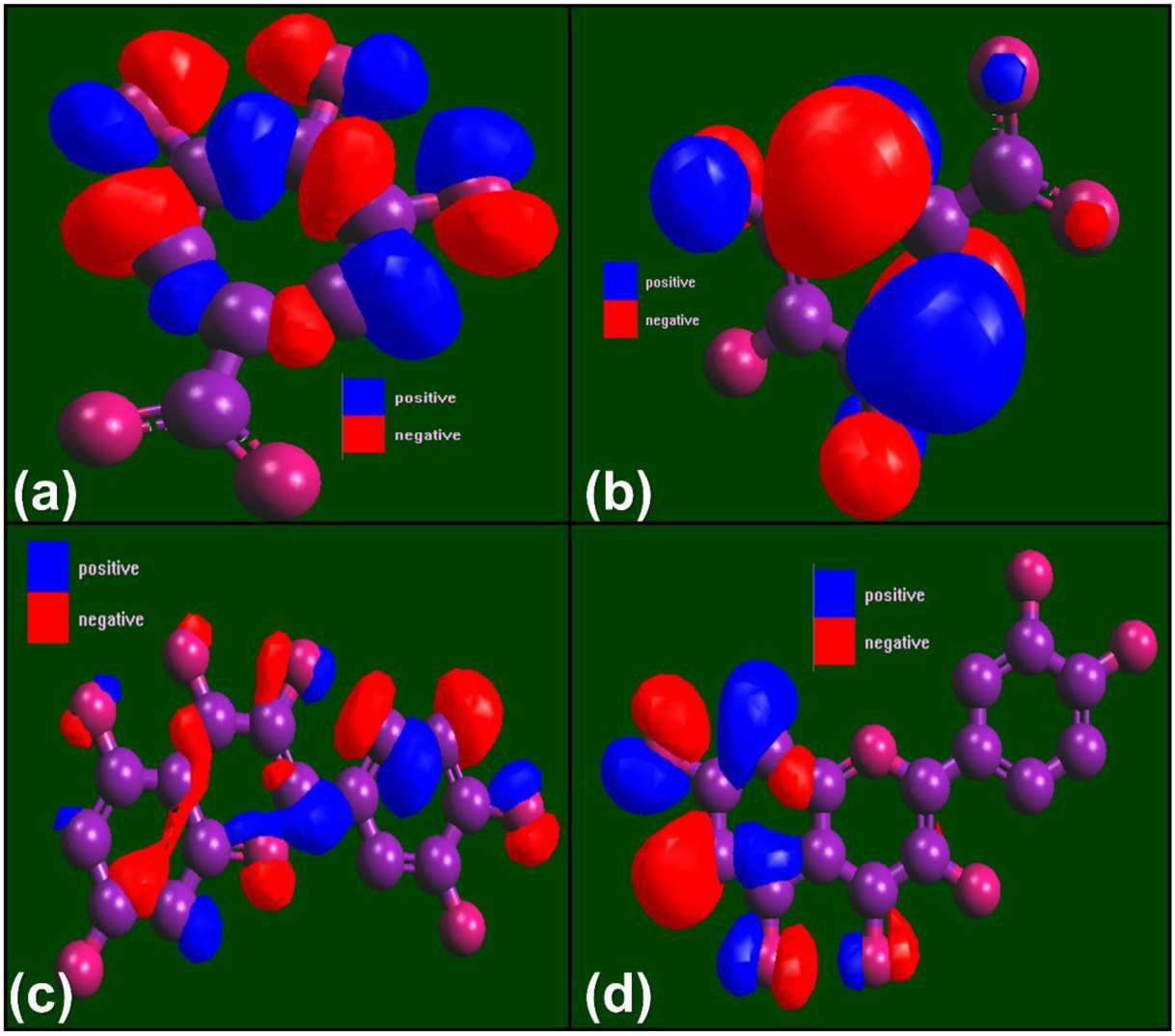

Fig. 4. (a–d):Molecules showing (a) Gallic acid- (E_{HOMO}), (b) Gallic acid- (E_{LUMO}), (c) Quercetin (E_{HOMO}), (d) Quercetin (E_{LUMO}).

where, Icorr0 -Al corrosion current density (which was obtained from instrument) without AgNPs and Icorr -Al corrosion current density with AgNPs. The morphology of Aluminium without and with 0.4 mg/L of AgNPs was screened by scanning electron microscopy (SEM) technique at an immersion time of 5 h.

3. Results and discussion

UV–visible spectroscopy technique is generally used for the analysis of structural and optical characters of nanoparticles. Synthesized silver nanoparticles were controlled by the alteration in colour of the combination of $AgNO_3$ and plant extract in proper proportions. The colour of the two mixtures were changed from green to yellow, then brown after around 30 min. These colour variations were due to the optical properties exhibited by silver nanoparticles. This was due to SPR peaks, the unique characteristic property shown by noble metals, observed when free moving electron of AgNPs interact with UV or Visible radiations.

According to Mie's theory of colloidal particles, AgNPs size and shape varies with different absorption bands. UV–Visible spectrum also shows anisotropic nature exhibited by two or three absorption bands, at 742 nm gives perfect triangular, as cited by Chen and Carroll, at 465 nm which indicates triangular shapes as in Chalmers and Griffiths and Farooq et al. Same time 333 nm associated with quadrupole resonance outside the plane. In present study it was found two major bands one at 280 nm another 450 nm. We also tried time gap of formation of AgNPs after adding of extract UV visible spectra were recorded each 5 min time interval. Interestingly there is not much shift in both peaks wavelengths. The well-defined SPR band is observed at 450 nm (shown in Fig. 5 a) for the synthesized silver nanoparticles. Absorbance at about 450 nm confirms the formation of AgNPs. SPR band increases with time, also evidence the formation of new AgNPs in the solution. This band also represents individual metal particle size and shape. Secondary phytomedicines of a leaf extract utilized to reduce and cap the AgNPs were identified by the Fourier transform infrared (FT-IR) spectroscopy. The FT-IR spectrum of AgNPs is shown in Fig. 5 b. The AgNPs showed the major absorption bands at 1068.7 cm^{-1}, 1462.91 cm^{-1}, 1740.50 cm^{-1}, 2853.27 cm^{-1}, 2952.22 cm^{-1}, 3011.13 cm^{-1}, and 3405.05 cm^{-1}. The absorption at 2224 cm^{-1} is associated with CH stretch (alkyl). The band around 1740.50 cm^{-1} is assigned for stretching vibration of –C = C-, and the band at 3011.13 cm^{-1} and 3405.05 cm^{-1} can be assigned for N–H/O–H vibration stretching which recommends that some polyphenolic compounds are attached to the silver nanoparticles. The formation of hybrid AgNPs might be due to these FT-IR bands of amine, alcoholic and carbonyl groups, needed for the capping of silver nanoparticles synthesized [10–12].

The XRD technique is used to confirm the crystalline/amorphous nature of newly synthesized AgNPs. The crystallite size (L) of green AgNPs was evaluated with the help of the Scherrer equation, as shown

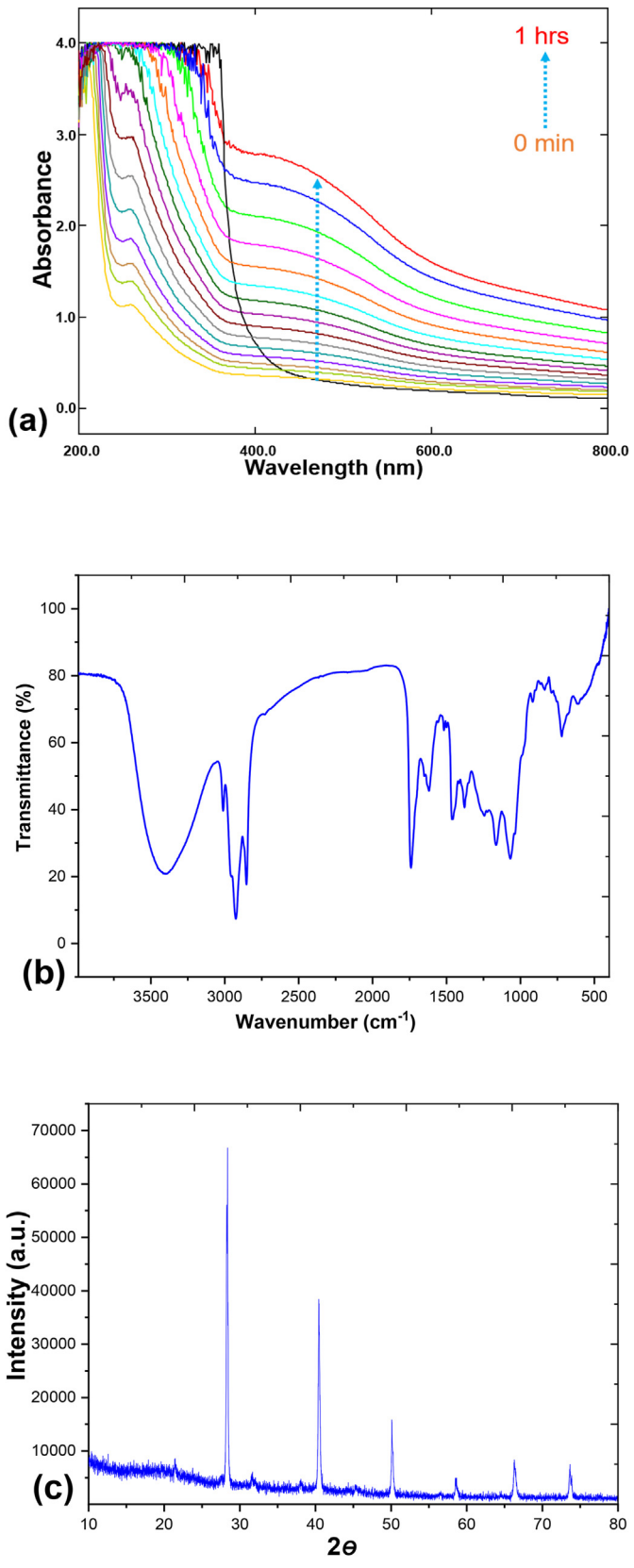

Fig. 5. (a–c): (a) UV–Visible spectrum, (b) FT-IR spectrum and (c) XRD results of AgNPs.

below:

$$L = \frac{B\lambda}{\beta cos\theta} \quad (4)$$

where, β - full-width half maximum of diffraction, B - Scherer constant, θ - Bragg's angle, and λ - wavelength.

The XRD pattern of AgNPs is shown in Fig. 5 d. X-ray diffraction (XRD) pattern of AgNPs shows well resolved and high-intensity peaks at 2Θ = 38.28°, 44, 64.36° and 77.12°, which indicates the crystal lattice nature of AgNPs. The literature study shows that the standard peaks for AgNPs are at 2Θ = 38.162°, 44.597°, and 77.544° [13–15]. This confirms the formation of new silver nanoparticles by Ag + ions to Ag with the help of EC extract. The spectrum at (111), (200) and (311) planes respectively indicate the Face Cantered Cubic (FCC) and crystalline structure of the silver nanoparticles. A high-intensity peak observed at 2Θ = 38.28° showing that, favoured orientation of AgNPs is (111) plane [12,15–17]. From the Scherrer equation, the average particle size of AgNPs ranged between 16 and 65 nm in diameter.

Constituent elemental analysis with an abundance of biologically synthesized AgNPs was found using Energy Dispersive X-ray (EDX) as represented in Fig. 6. The purity and chemical composition of AgNPs reveal a significant percentage of silver metal initiated with other elements. As organic capping agents, relative compositions of oxygen, silicon, and potassium with silver bind to the surface of AgNPs. The distribution of particle size pattern for AgNPs, investigated with the help of HRTEM images by measuring the diameters of at least 100 particles. The results of HRTEM are depicted in Fig. 6. HRTEM images confirm the spherical Ag particle structures. The AgNPs nanoparticle average size ranges from 15 to 25 nm. The maximum particle size distributions in the diameter range 35–60 nm.

The study of the antibacterial activity of AgNPs is very much essential for numerous medical and packing applications. The results of antibacterial activity are shown in Fig. 7. It has antibacterial activity against *Staphylococcus aureus* and *Escherichia coli*, which are both Grampositive, round-shaped bacteria. In current study, gram-negative bacteria such as *E. coli* are depicted. In silver nanoparticles case, as the surface area increases, the number of atoms at the surface also increases. The high stability of nanoparticles indicates higher concentrations of phytochemicals are act as more efficient reducing agents. Fig. 6, images shown that, there is optimum antimicrobial activity. Zone of inhibition is optimum at 500 and 1000 μg clear zone. On this large surface area, small microbes got trapped easily and interacted with silver nanoparticles [49]. Ultra-smaller size of silver nanoparticles, which would be around 200 times smaller than the bacterial sizes create an electrostatic attractive force between the microbial surface and nanoparticles, which make them inactive by trapping with vital enzymes containing thiol groups, leading to disturb the regular functioning of the bacterial cells and further to cause death of cell [50] and their antibacterial efficiency increase [48–52]. It also depends on the shape of the synthesized silver nanoparticles [53] and these all aspects helps to explain the antibacterial activity [17–20]. The activity is more noticeable for gram-negative bacteria, with a zone of inhibition measured shown to be good with bacteria *Escherichia. coli* at 1000 μg/ml [54–57]. Same time results also shown that AgNPs have no vital antibacterial effect on *Staphylococcus aureus* strain [16,18,19].

The precise mechanism to cause antimicrobial effect for silver nanoparticles is still a debated topic. The electrostatic interaction can be another possible reason for this. When predicting the antibacterial efficiency of silver nanoparticles, the medium, area, and shape are all important considerations. Additionally, when the free radicals formed by the silver nanoparticles encounter bacteria, the cell membrane is damaged, resulting in the bacteria dying because of the porous cell membrane. Once membrane ruptured the bacterial cell and its organelles

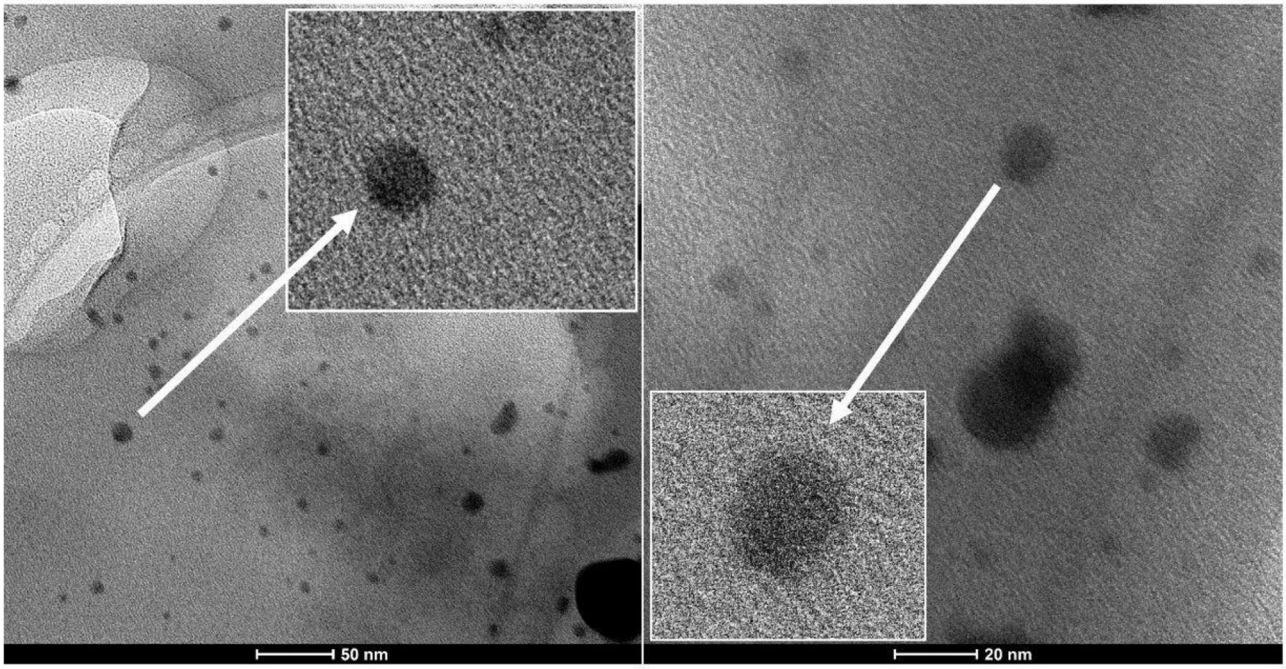

Fig. 6. HRTEM images of AgNPs.

eventually die which was schematically shown in Fig. 7 (b). Silver nanoparticles were found in the vacuole and on the cell wall, and they were found to be toxic. They inhibited cell division and caused damage to the bacteria cell envelope as well as their contents and it will restrict growth of bacteria [58,59].

The technique of atomic absorption spectroscopy (AAS) was used to investigate the effect of AgNPs on the anti-corrosion of Al in the experimental solution, which was found to be beneficial. 10 h at 303 °C were spent submerging the pre-weighed Al coupon in 1 M HCl solution without and with AgNPs for the duration of the experiment. Afterwards, the Al electrode is removed from the 1 M HCl solution and the weight loss is recorded using a digital analytical balance, which is connected to the computer. The results of the AAS are presented in Table 4, which includes. The table showed the robust adherence of the AgNPs on the Al surface in the experimental solution. From Table 4, the Al weight loss was reduced with the addition of AgNPs at concentrations of 1 mg/L, 2 mg/L, 3 mg/L, and 4 mg/L in 1 M HCl solution. The increase in the absorption of AgNPs results in an increase in the surface coverage of green nanoparticles over the Al surface in the experimental solution, which results in an increase in the protection rate. The adsorption of AgNPs over the Al surface generates a hedge for mass and charge movement, reducing the interaction between the HCl solution of concentration 1 M and the Al surface. The presence of AgNPs film on the Al surface blocks the Al surface disintegration. The protection efficiency of AgNPs on the Al surface could be associated with the adsorption of electron-rich elements on the empty or partially filled orbits of Al in the 1 M HCl solution. Therefore, enhancing the stability of newly generated bonds with the green nanoparticles [60–62].

AC impedance spectroscopy provides information about the kinetics of reactions at the aluminium/1 M HCl solution interface. Fig. 8 (a) represents the Nyquist curves obtained from the inhibition of Al corrosion by using the concentrations of 1 mg/L, to 4 mg/L of EC-AgNPs. The Nyquist readings for the different readings are shown in Table 5. The Nyquist plots (impedance curves) of the protected system are not different from the unprotected system except in terms of the diameter of the depressed semi-circle.

The Nyquist plots in Fig. 8 (a) show that the presence and absence of EC AgNPs(Only extract) is not a perfect semicircle due to frequency dispersion. The values of charge transfer capability are directly proportional to the concentration of AgNPs in the sample solution. With an increase in the concentration of the 1 mg/L to 4 mg/L of, the charge transfer resistance values improve and the rate of aluminium corrosion decreases, respectively. The fact that the radius of the depressed semicircle increases with an increase in the dosage of AgNPs is strong evidence that the dissolution process of Al in the 1 M HCl solution is prevented by the compound. The formation of a barrier protective layer on the Al surface significantly reduces the rate of disintegration of the Al surface. It is clear from this table that the values of charge transfer resistance are inversely proportional to the concentration of AgNPs in solution. The increase in charge transfer resistance values as the concentration of AgNPs increases is a clear indication of the anticorrosive behaviour of AgNPs over the Al electrode surface in the 1 M HCl solution, as demonstrated by the increase in charge transfer resistance values. It can be seen from the Chi-square (2) and surface heterogeneity factor values that the proposed circuit is well-suited for impedance measurements.

The polarization plots for Aluminium in the solution of 1 M HCl containing four different dosages of AgNPs are shown in Fig. 8 (b). The results are tabulated in Table 6. It is detected that; the introduction of green nanoparticles had a significant influence on the aluminium corrosion current density values and higher at higher concentration of AgNPs low aluminium corrosion current density value is obtained. The surface area of Al covered by AgNPs species enhances with the rise in AgNPs, which shows the aluminium protection is mainly due to the green nanoparticle adsorption over the Al surface. AgNPs formation layer over the surface of the Al surface, which restricts the interaction of Al with solution medium (Fig. 9). In which the silver nanoparticles here acting as anticorrosion agent. Further, no substantial change in the E corr, anodic

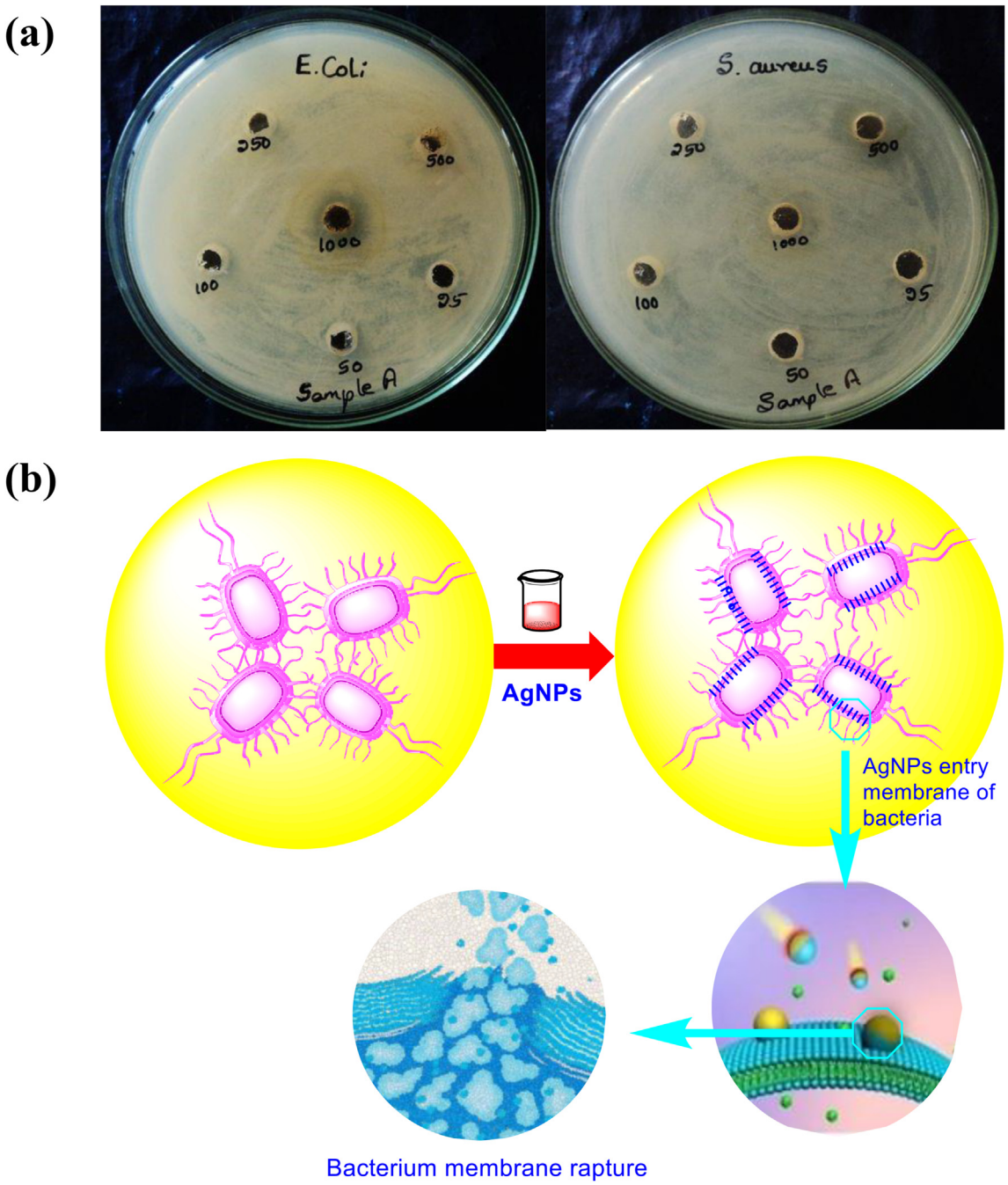

Fig. 7. **(a)** Plates showing Antibacterial activity of EC extract and AgNPs; **(b)** Figure Schematic representation of antibacterial activity of AgNPs.

Table 4
Atomic Absorption Spectroscopic results.

Concentration (mg/L)	Weight loss of Aluminium in grams after 10 h immersion period	Protection efficiency (%) with Std deviation
Bare	30×10^{-3}	
0.1	1.8×10^{-3}	94.000 ± 0.031%
0.2	1.4×10^{-3}	95.333 ± 0.027%
0.3	8×10^{-4}	97.333 ± 0.015%
0.4	1×10^{-4}	99.666 ± 0.007%

or cathodic Tafel slope values shows the mixed corrosion inhibition property of the AgNPs over the aluminium surface in the 1 Molar HCl solution [9,23].

The morphology of Al in was examined by SEM technique to assess the surface damage and protection after removed from the hydrochloric acid and AgNPs inhibited solutions. As shown in Fig. 9C, the topography of Al surface in 1 M HCl solution without and with the optimal concentration of AgNPs differs depends on the concentration of AgNPs used. In absence of AgNPs, the Al surface suffers severe damage because of the attack of H^+ and Cl^- ions on the Al surface. In contrast, the undulation and surface pitting were significantly reduced when the AgNPs were used at their maximum concentration (0.4 mg/L). When Al is exposed to 1 M HCl, ECNPs adsorb on the surface of the metal, resulting in a variation in the SEM topography of Al. This confirms the protective role of ECNPs.

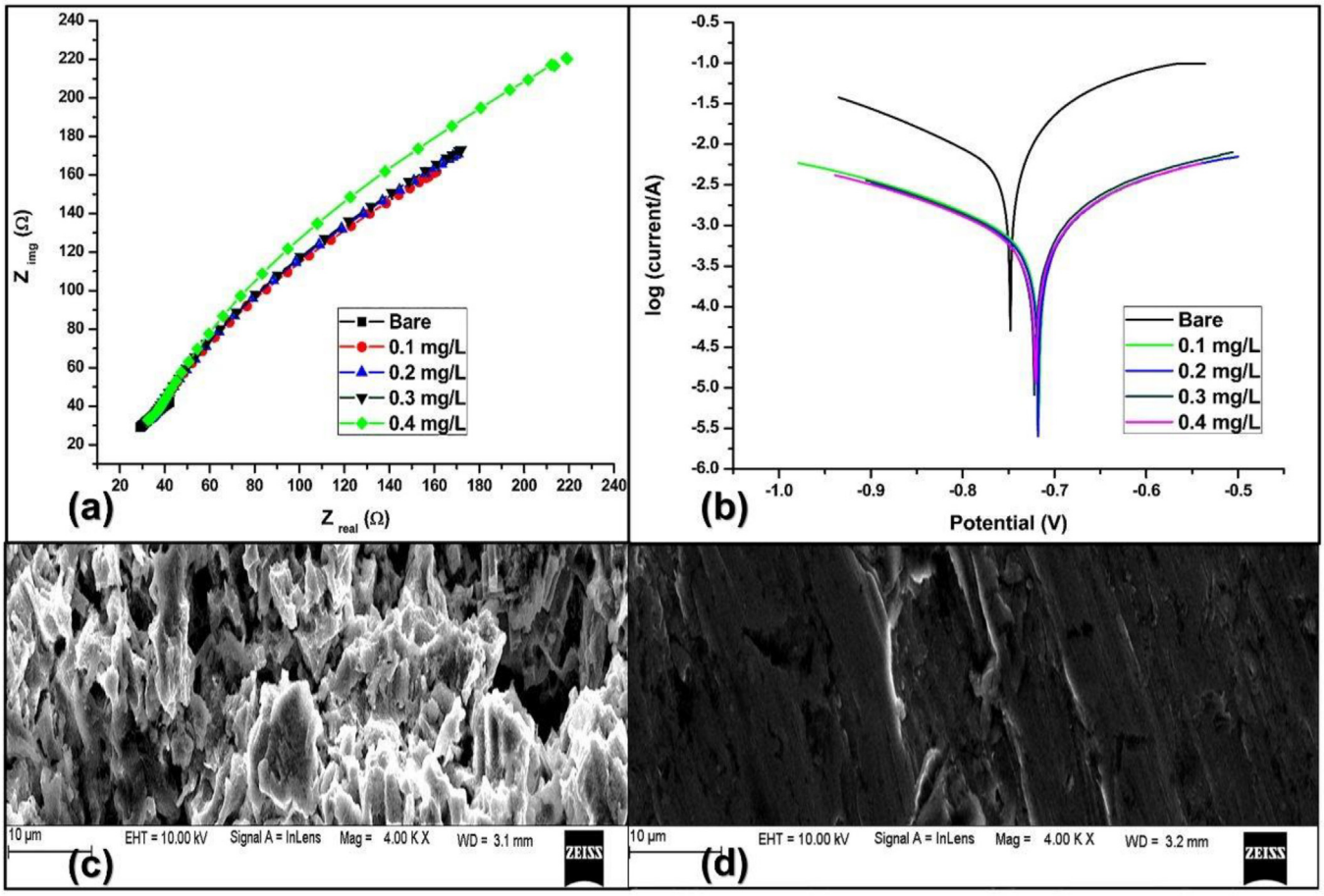

Fig. 8. (a–d) (a) Nyquist plots in the absence and presence of corrosion inhibitor, (b) Tafel plots without and with corrosion inhibitor, (c & d) SEM images without and with silver nanoparticles.

Table 5
Impedance spectroscopy results.

Concentration (mg/L)	n	R_{ct} (Ω)	χ2	Inhibition efficiency with Std deviation
Bare	0.9174	13.35	0.00001817	
0.1	0.8863	168.4	0.00006510	92.072 ± 0.013%
0.2	0.8790	176.9	0.00004471	92.453 ± 0.009%
0.3	0.8846	181.4	0.00009282	92.640 ± 0.043%
0.4	0.7953	231.7	0.00004452	94.238 ± 0.007%

Fig. 8 depicts a schematic representation of the inhibition of Al corrosion in a 1 M HCl solution by Gallic acid and Quercetin.

4. Conclusions

In present work successfully synthesized stable AgNPs by using green route from *Eichhornia Crassips* leaves extract and obtained sphere-like shape with sizes ranging from 16 to 65 nm. First time *Eichhornia crassips* extract was used for the synthesis of silver nanoparticles. They exhibit significantly effective antibacterial activity against *E. coli.* Additionally, anti-corrosion activity of EC-extract was carried out. The protection efficiency values obtained from the three techniques (AAS, Tafel plot, and impedance spectroscopy) and it was increased with the dosage of nanoparticle concentration. From the technique of AAS was obtained the highest possible protection efficiency value (99%). The AAS, Tafel plot, and impedance results are all correlated with surface morphological changes after using AgNPs which was observed by SEM. These novel properties of AgNPs demonstrate that the bio-waste *Eichhornia* plant can be used as a potential source for large scale synthesis of AgNPs with biological applications in the future.

Table 6
Results obtained from Tafel plot.

Concentration (mg/L)	Corrosion potential (E corr) (mV)	Anodic Tafel slope (V/dec)	Cathodic Tafel slope (V/dec)	Corrosion current (μA/cm^2)	Protection efficiency (%) with Std deviation
Bare	-777	0.003	6.392	55,700	
0.1	-717	5.251	4.719	1191	89.366 ± 0.017%
0.2	-718	5.415	4.703	1078	90.375 ± 0.005%
0.3	-722	5.535	4.738	1071	90.437 ± 0.007%
0.4	-720	5.494	4.717	1029	90.812 ± 0.009%

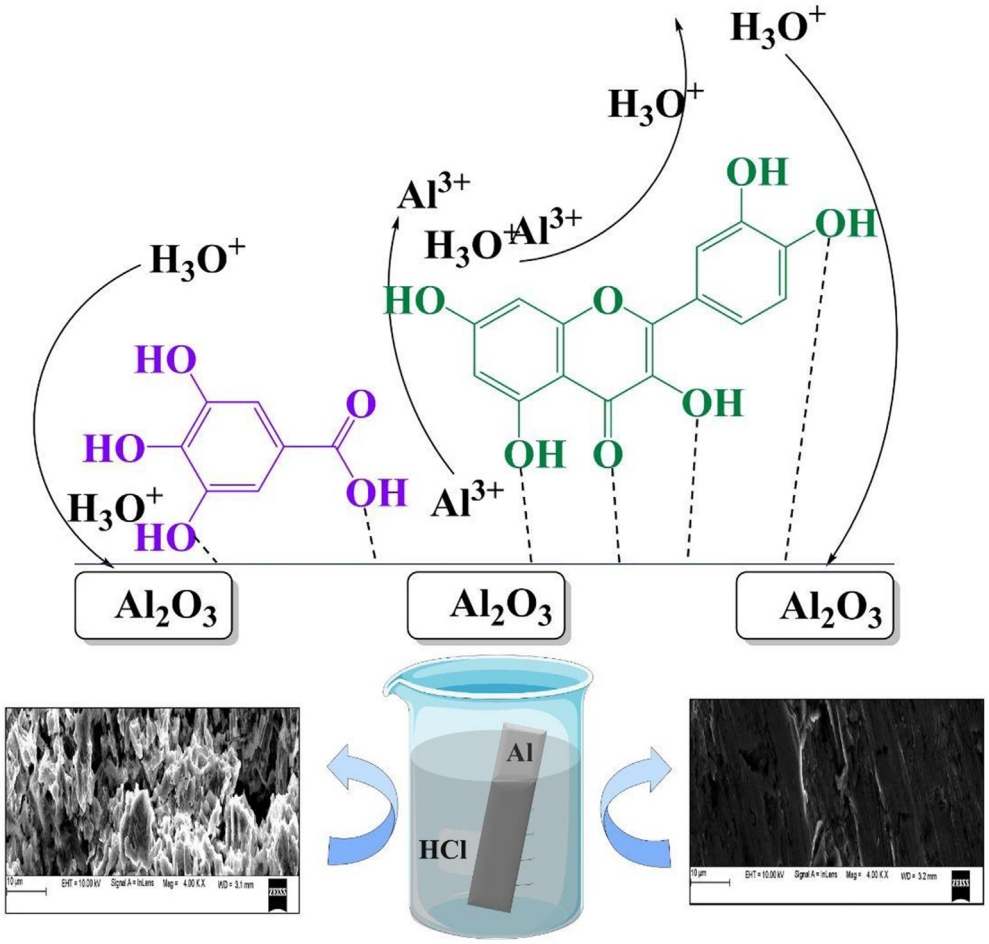

Fig. 9. Representation of inhibition of Al corrosion in 1 M HCl solution (0.4 mg/L of EC solution).

Declaration of competing interest

The authors declare that they have no known competing financial interests or personal relationships that could have appeared to influence the work reported in this paper.

Acknowledgements

The authors L. V. Hublikar, S. V. Ganachari, N. Raghavendra and N.R. Banapurmath acknowledge the Department of Chemistry & Alumni association of KLE Society's P C Jabin Science College, KLE Society Belagavi, and KLE Technological University (formerly known as B. V. Bhoomaraddi College of Engineering & Technology), for supporting research. The authors acknowledge the TEM Facility, funded by a "Thematic Projects in Frontiers of Nano S&T (TPF-Nano)" Nano-mission, GOVERNMENT OF INDIA project at Centre for Nano and Soft Matter Sciences, Bengaluru.

ABBREVATIONS

EC	*Eichhornia crassipes*
EC-AgNPs	*Eichhornia crassipes* extract silver nanoparticles
AgNPs	silver nanoparticles
NP's	Nanoparticles
UV/Vis	Ultraviolet–Visible spectroscopy
FTIR	Fourier-Transform Infrared Spectroscopy
XRD	X-ray Diffraction
SEM	Scanning electron microscopy
SEM-EDX	Scanning Electron Microscopy- Energy-dispersive X-ray spectroscopy
HRTEM	High-Resolution Transmission Electron Microscopy
E. coli	Escherichia. Coli
S. aureus	*Staphylococcus aureus*
$AgNO_3$	Silver nitrate
1 M HCl	One molar Hydrochloric acid
AAS	Atomic Absorption Spectroscopy - 0.01 N: 0.01 Normal
Al metal	Aluminium metal
OCP	open circuit potential
FCC	Face Centered Cubic E corr: Corrosion mg/L: milligram per litre

References

[1] R.K. Das, V.L. Pachapur, L. Lonappan, M. Naghdi, R. Pulicharla, S. Maiti, M. Cledon, L.M.A. Dalila, S.J. Sarma, S.K. Brar, Nanotechnol. Environ. Eng. 2 (2017) 18.
[2] S.V. Ganachari, N.R. Banapurmath, B. Salimath, J.S. Yaradoddi, A.S. Shettar, A.M. Hunashyal, A. Venkataraman, P. Patil, H. Shoba, G.B. Hiremath, in: L.M.T. Martínez, O.V. Kharissova, B.I. Kharisov (Eds.), "Synthesis Techniques for Preparation of Nanomaterials," *Handbook Of Ecomaterials*, Springer International Publishing, Cham, 2019, p. 83.
[3] S. Sim, N.K. Wong, Biomedical Reports 14 (2021) 1.
[4] A.S. Ali, Application of Nanomaterials in Environmental Improvement, IntechOpen, 2020.
[5] A.C. Gomathi, S.R. Xavier Rajarathinam, A. Mohammed Sadiq, S. Rajeshkumar, J. Drug Deliv. Sci. Technol. 55 (2020) 101376.
[6] A. Verma, M.S. Mehata, Journal of Radiation Research and Applied Sciences 9 (2016) 109.
[7] S.V. Ganachari, J.S. Yaradoddi, S.B. Somappa, P. Mogre, R.P. Tapaskar, B. Salimath, A. Venkataraman, V.J. Viswanath, in: L.M.T. Martínez, O.V. Kharissova, B.I. Kharisov (Eds.), "Green Nanotechnology for Biomedical, Food, and Agricultural Applications," *Handbook Of Ecomaterials*, Springer International Publishing, Cham, 2019, p. 2681.

[8] S.V. Ganachari, in: L.M.T. Martínez, O.V. Kharissova, B.I. Kharisov (Eds.), "Polymers for Energy Applications," *Handbook Of Ecomaterials*, Springer International Publishing, Cham, 2019, p. 3011.
[9] A.R.A. Scharnberg, A.C. de Loreto, A.K. Alves, Emerging Science Journal 4 (2020) 11.
[10] M.A. Hashem, S. Payel, M. Hasan, M.A. Momen, M.S. Sahen, HighTech and Innovation Journal 2 (2021) 99.
[11] S.V. Ganachari, R. Bhat, R. Deshpande, A. Venkataraman, BioNanoSci 2 (2012) 316.
[12] S. Ahmad, S. Munir, N. Zeb, A. Ullah, B. Khan, J. Ali, M. Bilal, M. Omer, M. Alamzeb, S.M. Salman, S. Ali, IJN 14 (2019) 5087.
[13] S. Dehghanizade, J. Arasteh, A. Mirzaie, Artificial Cells, Nanomedicine, and Biotechnology 46 (2018) 160.
[14] F. Mohammadi, M. Yousefi, R. Ghahremanzadeh, Advanced Journal of Chemistry-Section A 2 (2019) 266.
[15] V. Ravichandran, S. Vasanthi, S. Shalini, S.A.A. Shah, M. Tripathy, N. Paliwal, Results in Physics 15 (2019) 102565.
[16] F.K. Alsammarraie, W. Wang, P. Zhou, A. Mustapha, M. Lin, Colloids Surf. B Biointerfaces 171 (2018) 398.
[17] S.V. Ganachari, R. Deshpande, R. Bhat, N.V.S. Rao, D.S. Huh, A. Venkataraman, J. Bionanoscience 5 (2011) 107.
[18] A.U. Mokashi, S.V. Ganachari, J.S. Yaradoddi, R.P. Tapaskar, N.R. Banapurmath, A.S. Shettar, IOP Conf. Ser. Mater. Sci. Eng. 376 (2018), 012055.
[19] M.J. Mulvihill, E.S. Beach, J.B. Zimmerman, P.T. Anastas, Annu. Rev. Environ. Resour. 36 (2011) 271.
[20] A. Gour, N.K. Jain, Artificial Cells, Nanomedicine, and Biotechnology 47 (2019) 844.
[21] M. Akter, Md M. Rahman, A.K.M.A. Ullah, Md T. Sikder, T. Hosokawa, T. Saito, M. Kurasaki, J. Inorg. Organomet. Polym. 28 (2018) 1483.
[22] A.E. Mohammed, A. Al-Qahtani, A. Al-Mutairi, B. Al-Shamri, K. Aabed, Nanomaterials 8 (2018) 382.
[23] N. Raghavendra, J.I. Bhat, Period. Polytech. - Chem. Eng. 62 (2018) 351.
[24] G. Lakshmanan, A. Sathiyaseelan, P.T. Kalaichelvan, K. Murugesan, Karbala International Journal of Modern Science 4 (2018) 61–68.
[25] C.C. Gunnarsson, C.M. Petersen, Waste Manag. 27 (2007) 117.
[26] M.M. de O. Buanafina, M.F. Buanafina, S. Dalton, P. Morris, M. Kowalski, M.K. Yadav, L. Capper, PLoS One 15 (2020), e0240369.
[27] N. Kumar, V. Pruthi, Biotechnology Reports 4 (2014) 86.
[28] M.J. Khan, K. Shameli, A.Q. Sazili, J. Selamat, S. Kumari, Molecules 24 (2019) 719.
[29] M. Khatami, I. Sharifi, M.A.L. Nobre, N. Zafarnia, M.R. Aflatoonian, Green Chem. Lett. Rev. 11 (2018) 125.
[30] K.C. Hembram, R. Kumar, L. Kandha, P.K. Parhi, C.N. Kundu, B.K. Bindhani, Artif Cells Nanomed Biotechnol 46 (2018) S38.
[31] M.Q. Nasar, A.T. Khalil, M. Ali, M. Shah, M. Ayaz, Z.K. Shinwari, Medicina 55 (2019) 369.
[32] N. Raghavendra, J. Ishwara Bhat, J Bio Tribo Corros 4 (2017) 2.
[33] I. Fatimah, Z.H.V.I. Aftrid, Green Chem. Lett. Rev. 12 (2019) 25.
[34] A.A. Alfuraydi, S. Devanesan, M. Al-Ansari, M.S. AlSalhi, A.J. Ranjitsingh, J. Photochem. Photobiol. B Biol. 192 (2019) 83.
[35] M. Behravan, A. Hossein Panahi, A. Naghizadeh, M. Ziaee, R. Mahdavi, A. Mirzapour, Int. J. Biol. Macromol. 124 (2019) 148.
[36] S. Jogaiah, M. Kurjogi, M. Abdelrahman, N. Hanumanthappa, L.-S.P. Tran, Arabian Journal of Chemistry 12 (2019) 1108.
[37] G. Arya, R.M. Kumari, N. Gupta, A. Kumar, R. Chandra, S. Nimesh, Artificial Cells, Nanomedicine, and Biotechnology 46 (2018) 985.
[38] V. Kumar, S. Singh, B. Srivastava, R. Bhadouria, R. Singh, Journal of Environmental Chemical Engineering 7 (2019) 103094.
[39] B. Mousavi, F. Tafvizi, S. Zaker Bostanabad, Artificial Cells, Nanomedicine, and Biotechnology 46 (2018) 499.
[40] C. Singh, J. Kumar, P. Kumar, B.S. Chauhan, K.N. Tiwari, S.K. Mishra, S. Srikrishna, R. Saini, G. Nath, J. Singh, Biotechnol. Biotechnol. Equip. 33 (2019) 359.
[41] F. Erci, R. Cakir-Koc, I. Isildak, Artificial Cells, Nanomedicine, and Biotechnology 46 (2018) 150.
[42] M. Hamelian, M.M. Zangeneh, A. Amisama, K. Varmira, H. Veisi, Appl. Organomet. Chem. 32 (2018) e4458.
[43] J.A. Rorong, S. Sudiarso, B. Prasetya, J. Polii-Mandang, E. Suryanto, AGRIVITA, Journal of Agricultural Science 34 (2012) 152.
[44] A.V.A. David, R. Arulmoli, S. Parasuraman, Phcog. Rev. 10 (2016).
[45] P. Lalitha, S.K. Sripathi, P. Jayanthi, Natural Product Communications 7 (2012), 1934578X1200700939.
[46] Res. J. Chem. Sci. 9 (2019) 1.
[47] A. Nayar, The Metals Databook, McGraw-Hill, 1997.
[48] M. Stern, A.L. Geary, J. Electrochem. Soc. 104 (1957) 56.
[49] Y.A. Yugay, R.V. Usoltseva, V.E. Silant'ev, A.E. Egorova, A.A. Karabtsov, V.V. Kumeiko, S.P. Ermakova, V.P. Bulgakov, Y.N. Shkryl, Carbohydr. Polym. 245 (2020) 116547.
[50] N.U. Islam, K. Jalil, M. Shahid, A. Rauf, N. Muhammad, A. Khan, M.R. Shah, M.A. Khan, Arabian Journal of Chemistry 12 (2019) 2914.
[51] N. Raghavendra, J. Ishwara Bhat, Journal of King Saud University - Engineering Sciences 31 (2019) 202.
[52] J. Singh, A.S. Dhaliwal, Anal. Lett. 52 (2019) 213.
[53] S. Mathew, A. Prakash, E.K. Radhakrishnan, Inorganic and Nano-Metal Chemistry 48 (2018) 139.
[54] M.L. Guimarães, F.A.G. da Silva, M.M. da Costa, H.P. de Oliveira, Appl. Nanosci. 10 (2020) 1073.
[55] R.S. Jones, R.R. Draheim, M. Roldo, Appl. Sci. 8 (2018) 673.
[56] S. Sumitha, S. Vasanthi, S. Shalini, S.V. Chinni, S.C.B. Gopinath, P. Anbu, M.B. Bahari, R. Harish, S. Kathiresan, V. Ravichandran, Molecules 23 (2018) 3311.
[57] A. Roy, O. Bulut, S. Some, A.K. Mandal, M.D. Yilmaz, RSC Adv. 9 (2019) 2673.
[58] K. Chand, M.I. Abro, U. Aftab, A.H. Shah, M.N. Lakhan, D. Cao, G. Mehdi, A.M.A. Mohamed, RSC Adv. 9 (2019) 17002.
[59] A.G. Femi-Adepoju, A.O. Dada, K.O. Otun, A.O. Adepoju, O.P. Fatoba, Heliyon 5 (2019), e01543.
[60] G.A. Otunola, A.J. Afolayan, Biotechnol. Biotechnol. Equip. 32 (2018) 724.
[61] R. Vijayan, S. Joseph, B. Mathew, Artificial Cells, Nanomedicine and Biotechnology 46 (2018) 861.
[62] N. Raghavendra, Chemistry Africa 3 (2020) 21.
[63] P.D. Sarvalkar, R.R. Mandavkar, M.S. Nimbalkar, et al., Sci. Rep. 11 (2021) 16934.